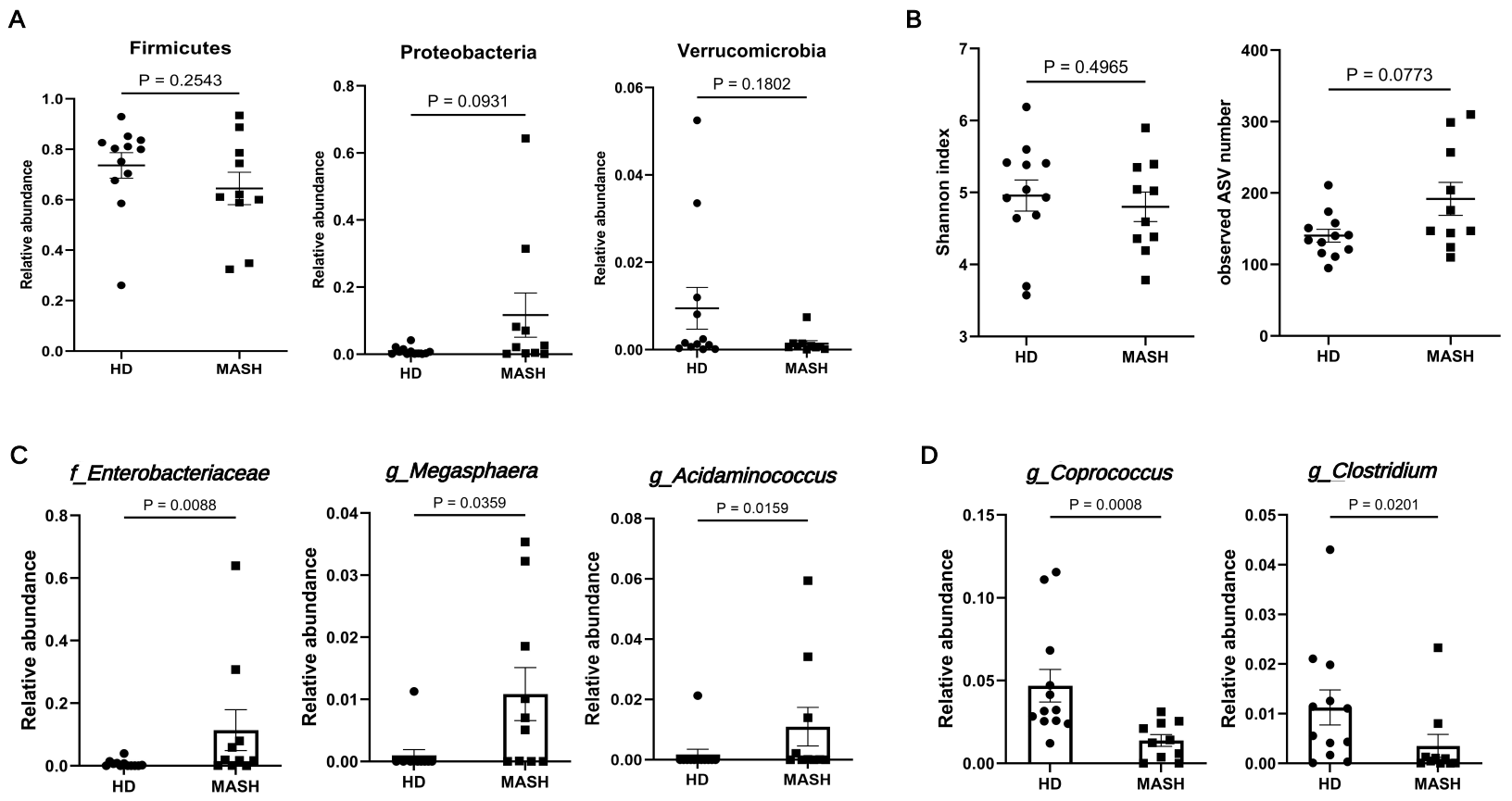

Supplement figure 1

A

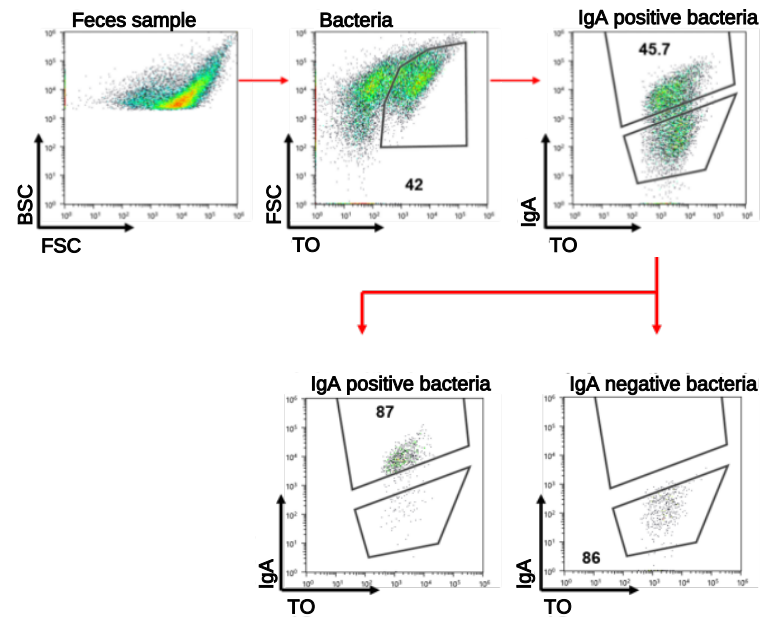

B

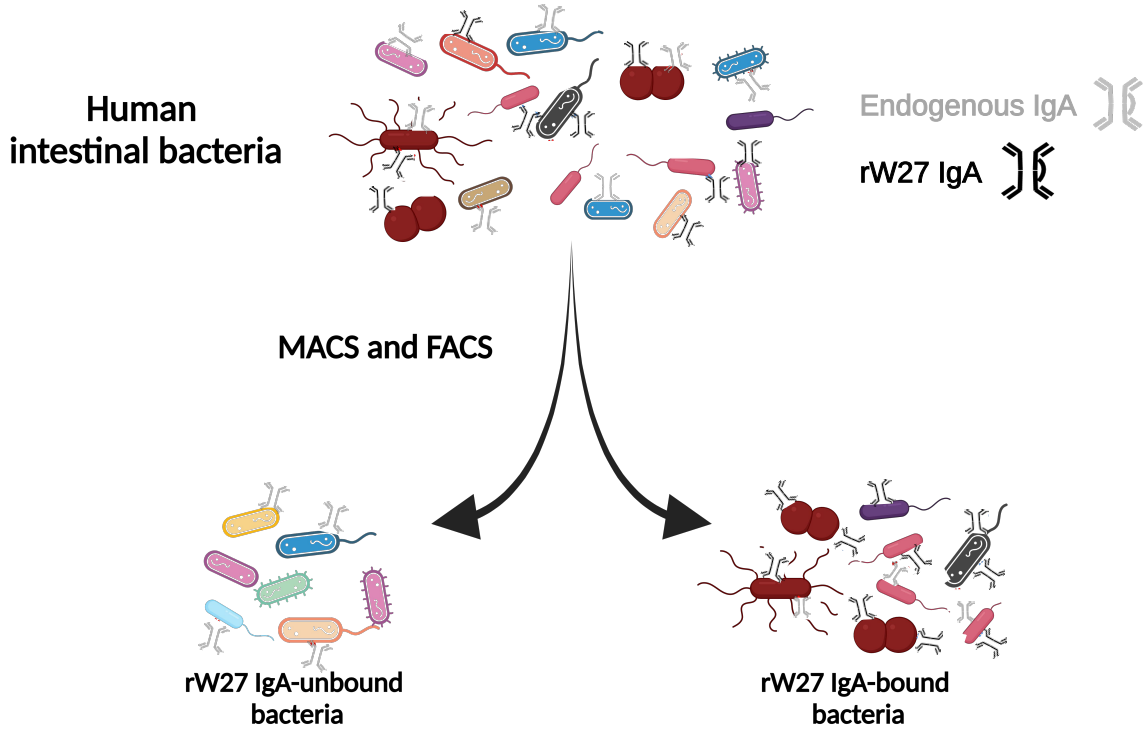

C

$$IgA^{+}_{\text{taxon abundance}} = IgA^{+}_{\text{relative abundance}} \times \text{IgA binding ability} / 100$$

$$IgA^{-}_{\text{taxon abundance}} = IgA^{-}_{\text{relative abundance}} \times (1 - \text{IgA binding ability} / 100)$$

$$\text{IgA index} = - \frac{[\log(IgA^{+}_{\text{taxon abundance}}) - \log(IgA^{-}_{\text{taxon abundance}})]}{[\log(IgA^{+}_{\text{taxon abundance}}) + \log(IgA^{-}_{\text{taxon abundance}})]}$$

D

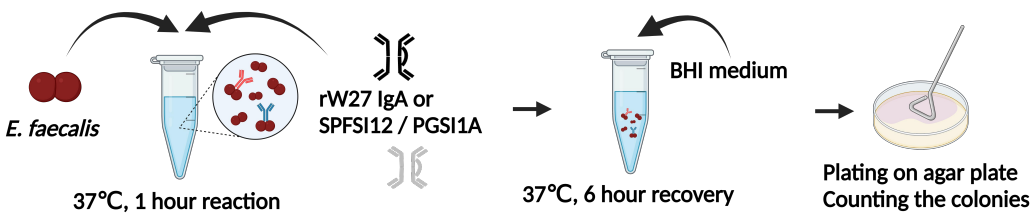

Supplement figure 2

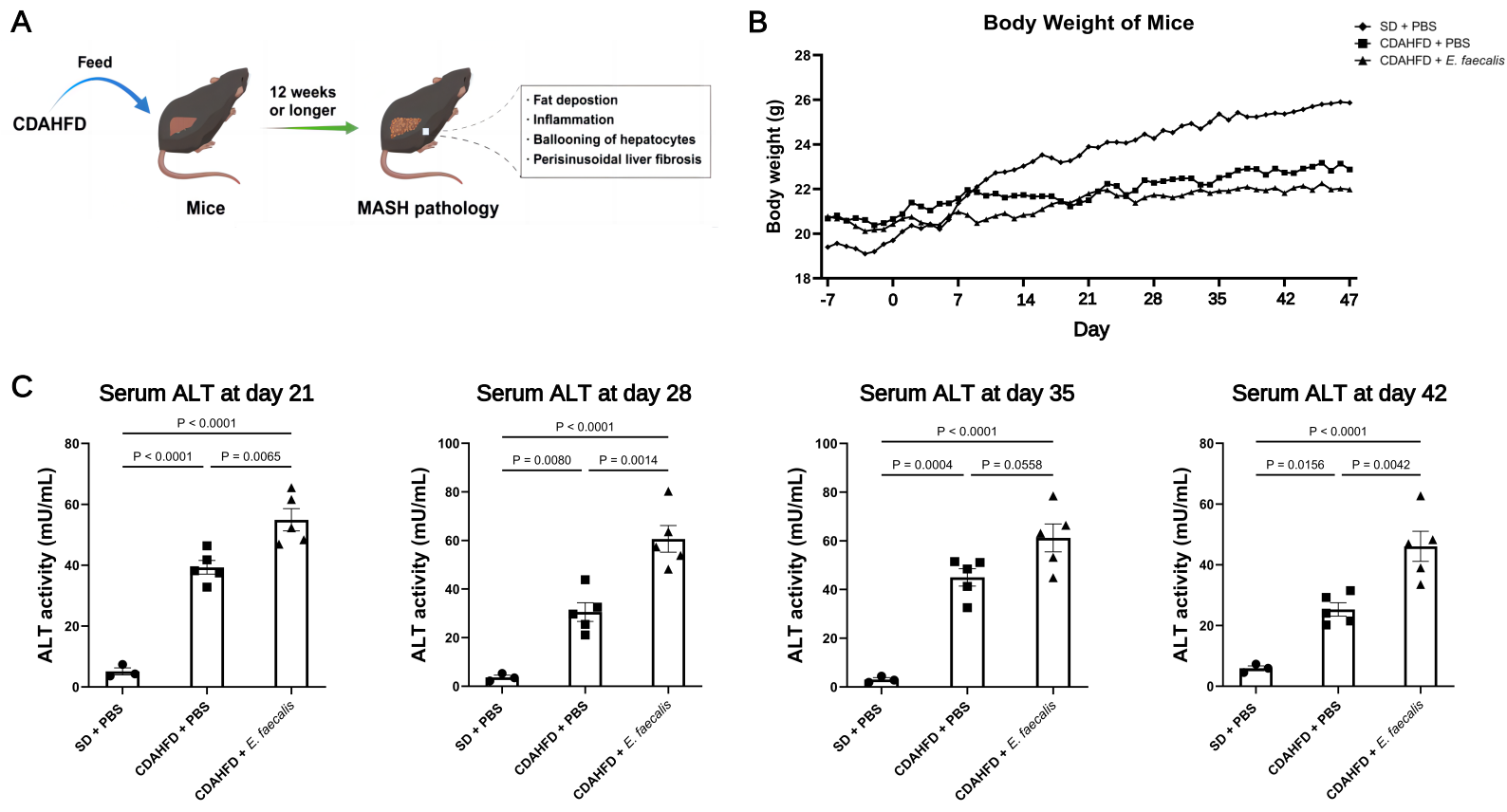

Supplement figure 3

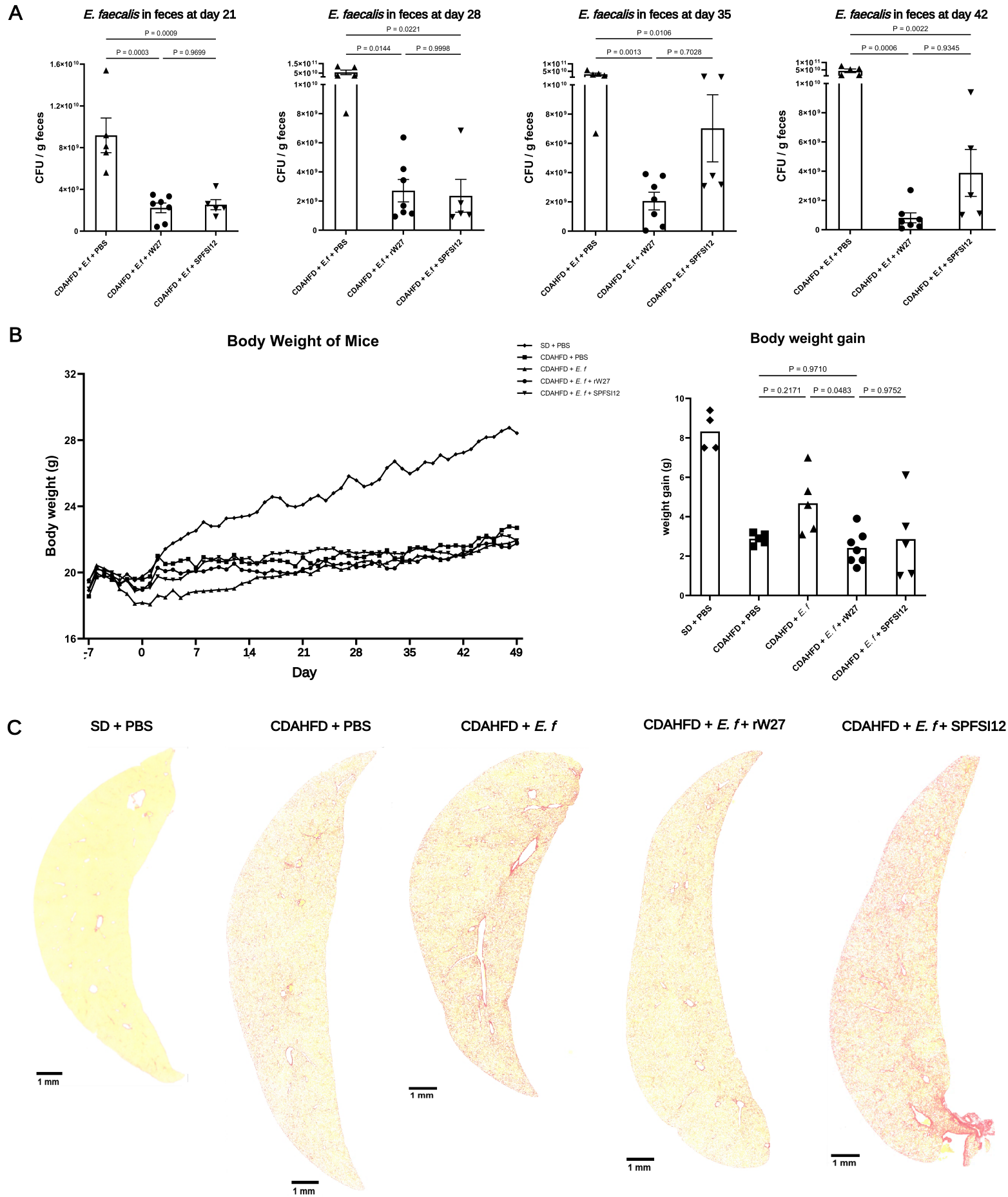

Supplement figure 4

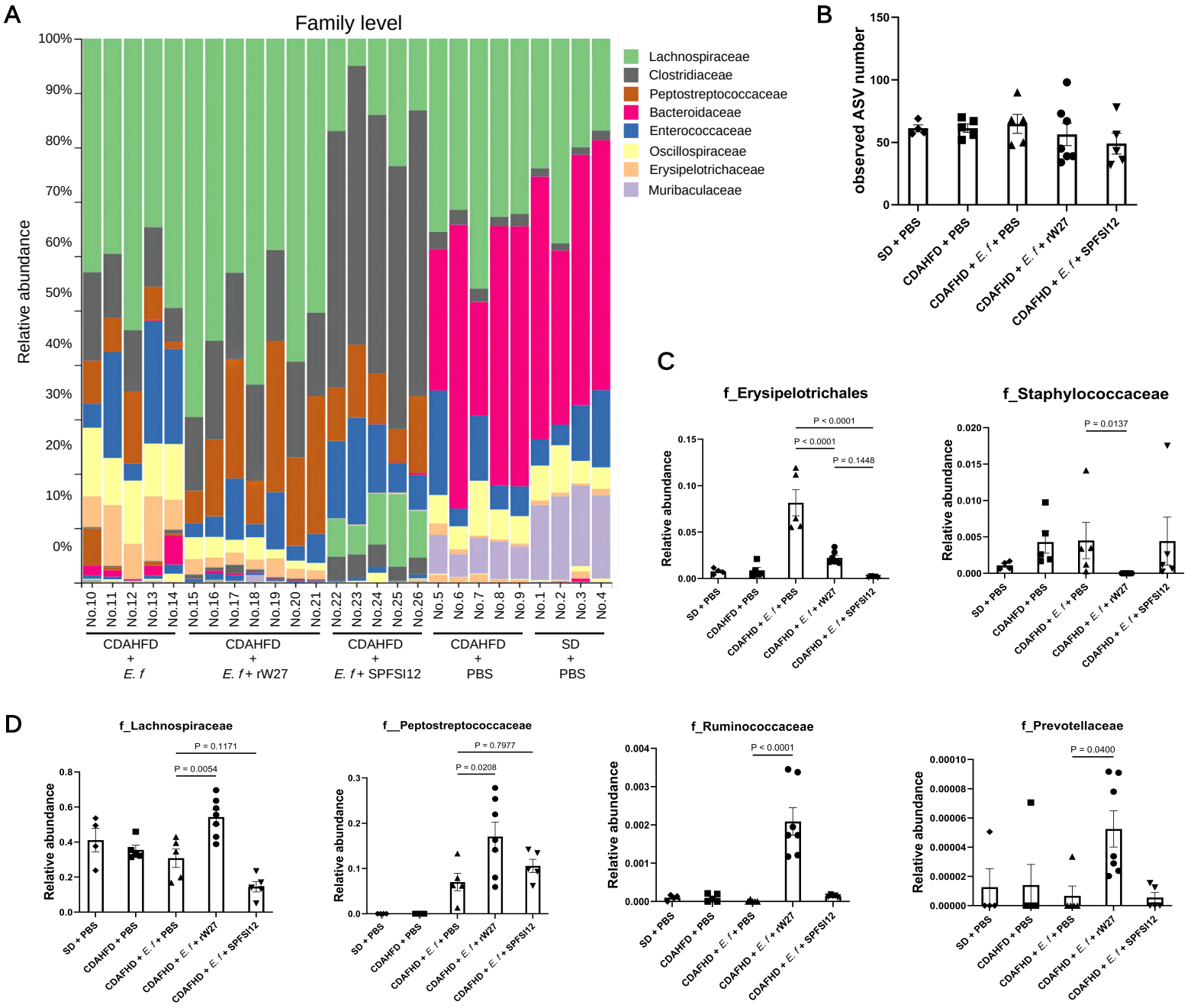

Supplement figure 5

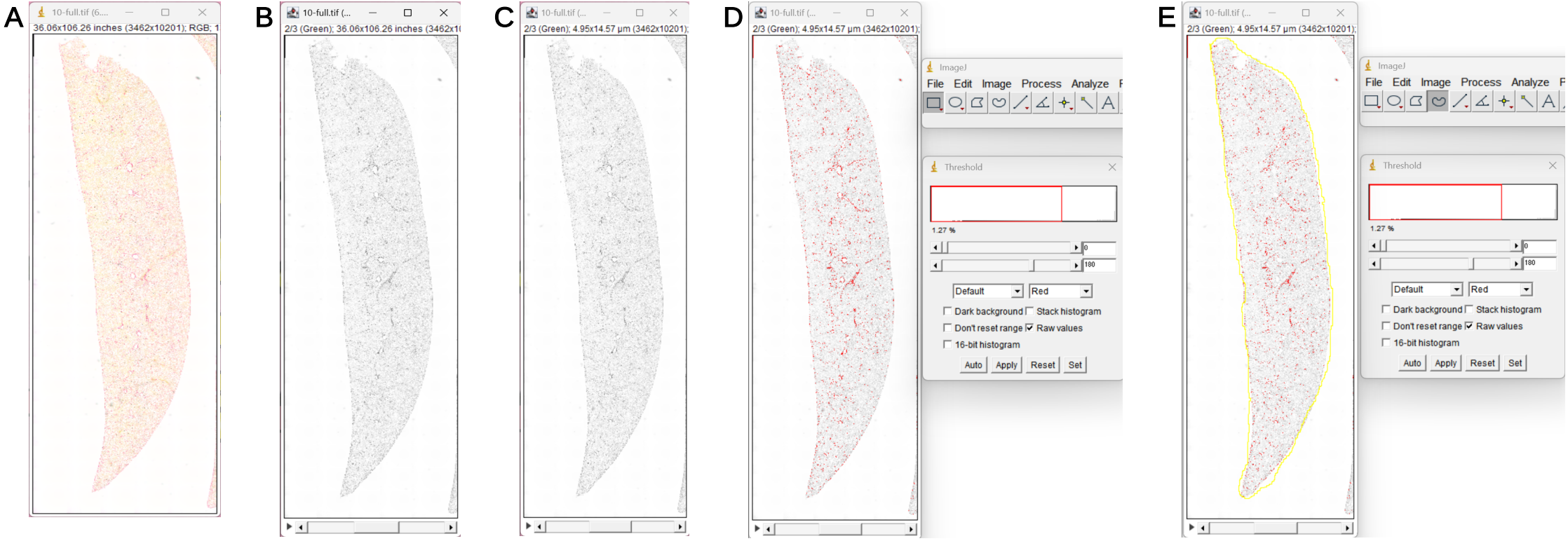

Supplement figure 6

Supplementary Figures

rW27 IgA alleviates *Enterococcus faecalis*-promoted CDAHFD-induced MASH in mice by attenuating the liver fibrosis

Xiujie Chen[1,2], Keishu Takahashi[1], Genta Furuya[1], Naoki Morita[1], Ryutaro Tamano[1],

Peng Gao[1], Noriho Iida[3], Yuki Sugiura[4], Rei Maeda[4], and Reiko Shinkura[1,2*],

[1]Institute of Quantitative Biosciences, The University of Tokyo, Tokyo, Japan

[2]Graduate School of Frontier Sciences, The University of Tokyo, Tokyo, Japan

[3]Department of Gastroenterology, Graduate School of Medical Sciences, Kanazawa University, Kanazawa, Japan

[4]Center for Cancer Immunotherapy and Immunobiology, Graduate School of Medicine, Kyoto University, Kyoto, Japan

* Address correspondence to Reiko Shinkura, Laboratory of Immunology and Infection Control, Institute for Quantitative Biosciences, The University of Tokyo, 1-1-1 Yayoi, Bunkyo-ku, Tokyo 113-0032, Japan; e-mail rshinkura@iqb.u-tokyo.ac.jp

Supplementary Figure 1

Alterations in gut microbiota composition and diversity in MASH Patients compared with HD

(A) Relative abundance of gut microbiota composition at the phylum level in MASH patients and HD. (B) Comparison of gut microbiota diversity between MASH patients and HD. Results are presented by Shannon diversity index and Observed ASV number. (C) Relative abundance comparison of the bacteria taxa enriched in MASH patients. (D) Relative abundance comparison of the bacteria taxa enriched in HD. Statistical analysis was performed by the Mann-Whitney U test. $P < 0.05$ was considered statistically significant. Data are presented as mean ± SEM. (n = 12 for the HD group, and n = 10 for the MASH patients' group).

Supplementary Figure 2

FACS-based separation, quantification, and functional assessment of IgA-binding gut bacteria

(A) FACS gating strategy for separating bacteria into IgA-bound and -unbound fractions. The mouse-derived monoclonal IgA used in the analysis was biotinylated. The results when no antibody was added were used as a negative control. (B) Strategy for separating and recovering rW27 IgA-bound and -unbound bacteria by FACS. rW27 IgA is shown in black and endogenous IgA in grey. (C) Method of calculating the IgA index. (D) Protocol for the growth inhibition experiment of *E. faecalis*.

Supplementary Figure 3

Establishment of the CDAHFD-induced MASH model and associated physiological changes in mice

(A) The MASH disease induction by the CDAHFD diet and the minimum time required for induction. Data were provided by the manufacturer Research Diet®. (B) Body weight changes in mice. (C) Serum ALT levels in mice were monitored weekly from week 3 (day 21) to week 6 (day 42). Statistical analysis was performed by one-way ANOVA followed by Tukey's multiple comparisons test. Data are presented as mean ± SEM, expect for body weight ratio (data are presented as mean). $P < 0.05$ is considered statistically significant. (*n*=3 for SD + PBS group, *n*=5 for CDAHFD + PBS group, and *n*=5 for CDAHFD + *E. faecalis* group)

Supplementary Figure 4

Dynamics of *E. faecalis* colonization, physiological changes, and liver fibrosis in MASH mice

(A) Comparison of the CFU number of *E. faecalis* in mouse feces every week from week 3 (day 21) to week 6 (day 42) as assessed by selective agar. (B) Body weight changes and gains in mice. (C) Representative photos of Sirius Red staining for each group at the endpoint, week seven. The photos are presented as full-size slides. Scare bar: 1 mm. Statistical analysis was performed by one-way ANOVA followed by Tukey's post-hoc test. Data are presented as mean ± SEM expect the body weight ratio (data are presented as Mean), with $P < 0.05$ considered statistically significant. (*n*=4 for SD + PBS group; *n*=5 for CDAHFD + PBS group; *n*=5 for CDAHFD + *E. faecalis* group; *n*=7 for CDAHFD + *E. faecalis* + rW27 group; *n*=5 for CDAHFD + *E. faecalis* + SPFSI12 group)

Supplementary Figure 5

Gut microbiota profiles in response to *E. faecalis* colonization and rW27 IgA treatment

(A) Comparison of the gut microbiota of mice at the endpoint of experiment (day 49) at the family level. (B) Comparison of gut microbiota diversity among the five groups. Results are presented by observed ASV number. (C) Relative abundance comparison of bacterial taxa enriched in the *E. faecalis*-fed group. (D) Relative abundance comparison of bacterial taxa enriched in the rW27 IgA-treated group. Statistical analysis was performed by one-way ANOVA followed by Tukey's multiple comparisons test. Data are presented as mean ± SEM, with $P < 0.05$ considered statistically significant. (*n*=4 for SD + PBS group, *n*=5 for CDAHFD + PBS group, *n*=5 for CDAHFD + *E. faecalis* group, *n*=7 for CDAHFD + *E. faecalis* + rW27 group, and *n*=5 for CDAHFD + *E. faecalis* + SPFSI12 group)

Supplementary Figure 6

Semi-quantitative analysis of liver fibrosis by Sirius Red staining using ImageJ

(A) Sirius Red-stained whole slide images were imported into ImageJ (version 1.54). (B) Each image was split into RGB stacks, and the green channel was selected for analysis. (C) The image scale was set as follows: *distance in pixels* = 700, *known distance* = 1.00, *pixel aspect ratio* = 1.0, *unit of length* = μm. (D) The threshold was set to (0, 180) to detect the Sirius Red-positive (fibrotic) areas. (E) The surrounding portal vein regions were manually excluded, and the remaining area was selected for quantification. The percentage of the Sirius Red-positive area was measured for statistical analysis.

Supplementary Materials and Methods

Materials

Table 1. List of antibodies

Antibody	Manufacturer
UNLB-Goat anti-human IgA (Polyclonal)	2050-01, Southern Biotech, Birmingham,USA
Human IgA lambda Antibody	OASB00157, avivasysbio, San Diego, USA
AP-Goat anti-Human IgA (Polyclonal)	2050-04, Southern Biotech, Birmingham,USA
PE/Cyanine 7-Streptavidin	405206, Biolegend, San Diego, USA
PE-Goat anti-human IgA (Polyclonal)	2050-09, Southern Biotech, Birmingham,USA
FITC-Anti-CD11b (clone M1/70)	101206, Biolegend, San Diego, USA
PE-Anti-F4/80 (clone BM8)	123110, Biolegend, San Diego, USA

Table 2. Primer sequences for quantitative qPCR experiments

Name	Forward (5' → 3')	Reverse (5' → 3')
β-actin	CCAACCGTGAAAAGATGACC	CCAGAGGCATACAGGGACAG
Tnfα	TCCAGGCGGTGCCTATGT	CACCCCGAAGTTCAGTAGACAGA
Il1b	CTGCAAGAGACTTCCATCCAGTT	AAGTAGGGAAGGCCGTGGTT
Il6	TCAGGCAGGCAGTATCACTCA	GGAAGGTCCACGGGAAAGAC
Ccl2	TTAACGCCCCACTCACCTGC	GTGCTGAAGACCTTAGGGCA
Col1a1	CCCTGAAGTCAGCTGCATACACAAT	CCTACATCTTCTGAGTTTGGTGAT
Col4a1	CACCCATCTCTGGGGACAAC	GTTAGGGCACTGCGGAATCT
Acta2	CGACACTGCTGACAGAGGCACCA	ATAGGCACGTTGTGAGTCACACCA
Tgfb1	TGACGTCACTGGAGTTGTACGGC	GCCGGTTCATGTCATGGATGGT

Table 3. List of reagents and chemicals

Reagent	Manufacturer
10× Loading Buffer	Takara Bio Inc., Shiga, Japan
100 bp DNA ladder	Takara Bio Inc., Shiga, Japan
4 % paraformaldehyde (PFA)	Nacalai Tesque, Kyoto, Japan
Acetone	Nacalai Tesque, Kyoto, Japan
Agar powder	Nacalai Tesque, Kyoto, Japan
Agarose	Nacalai Tesque, Kyoto, Japan

Albumin, from bovine serum, fraction Ⅴ	FUJIFILM Wako Pure Chemical Corporation, Osaka, Japan
ALT Activity Assay	Merck KGaA, Darmstadt, Germany
Anti-PE microbeads	Miltenyi Biotec, Bergisch Gladbach, Germany
Cell viability kit	BD Biosciences, Franklin Lakes, NJ, USA
Chloroform	Nacalai Tesque, Kyoto, Japan
Crushing beads (DNA / RNA)	TOMY Digital Biology Co., Ltd., Tokyo, Japan
EDTA (5 μM)	Nacalai Tesque, Kyoto, Japan
EF agar broth	Shimadzu Corporation, Kyoto, Japan
EmeraldAmp (2× Premix)	Takara Bio Inc., Shiga, Japan
Eosin alcohol solution, acid extract	FUJIFILM Wako Pure Chemical Corporation, Osaka, Japan
Ethanol	Nacalai Tesque, Kyoto, Japan
FastGene Gel/PCR extraction kit	Nippon Genetics Co., Ltd., Tokyo, Japan
FastGene RNA premium kit	Nippon Genetics Co., Ltd., Tokyo, Japan
Fluoromount G	Invitrogen, Carlsbad, CA, USA
GAM broth	Nissui Pharmaceutical Co., Ltd., Tokyo, Japan
Gentamycin	Nacalai Tesque, Kyoto, Japan
Glycerol	Nacalai Tesque, Kyoto, Japan
Glycogen	Nacalai Tesque, Kyoto, Japan
Hematoxylin solution	Sigma-Aldrich, St. Louis, MO, USA
Hemin	Kasei Kogyo Co., Ltd., Tokyo, Japan
ISOGEN Ⅱ	Nippon Gene Co., Ltd., Tokyo, Japan
Isopropanol	Nacalai Tesque, Kyoto, Japan
Kanamycin sulfate	FUJIFILM Wako Pure Chemical Corporation, Osaka, Japan
LED stain G	LABTAS+, Tokyo, Japan
Liquid counting beads	BD Biosciences, Franklin Lakes, NJ, USA
L-methionine	Nacalai Tesque, Kyoto, Japan
Magnesium chloride	Nacalai Tesque, Kyoto, Japan
Methanol	Nacalai Tesque, Kyoto, Japan
Metronidazole	FUJIFILM Wako Pure Chemical Corporation, Osaka, Japan
mGAM broth	Nissui Pharmaceutical Co., Ltd., Tokyo, Japan
Microbeads-streptavidin	Miltenyi Biotec, Bergisch Gladbach, Germany
Milli-Q water	Merck KGaA, Darmstadt, Germany
MOUNT-QUICK AQUEOUS	Funakoshi Co., Ltd., Tokyo, Japan
Neomycin trisulfate salt hydrate	Sigma-Aldrich, St. Louis, MO, USA
Neopor	CLEA Japan, Inc., Tokyo, Japan
Normal rat serum	FUJIFILM Wako Pure Chemical Corporation, Osaka, Japan

Oil Red O staining powder	FUJIFILM Wako Pure Chemical Corporation, Osaka, Japan
Penicillin	Nacalai Tesque, Kyoto, Japan
Phenol:chloroform:isoamyl Alcohol=25:24:1	Nacalai Tesque, Kyoto, Japan
Phosphatase substrate	Sigma-Aldrich, St. Louis, MO, USA
Phosphate buffered saline (10x)	Nacalai Tesque, Kyoto, Japan
Picro Sirius Red staining kit	ScyTek Laboratories, Logan, UT, USA
Propidium iodide	BD Biosciences, Franklin Lakes, NJ, USA
RNA cartridge kit	Funakoshi Co., Ltd., Tokyo, Japan
Sodium azide	Nacalai Tesque, Kyoto, Japan
Sodium bicarbonate	Nacalai Tesque, Kyoto, Japan
Sodium carbonate	Nacalai Tesque, Kyoto, Japan
Sucrose	Nacalai Tesque, Kyoto, Japan
SYTO24	Invitrogen, Carlsbad, CA, USA
Thiazole orange	BD Biosciences, Franklin Lakes, NJ, USA
Tissue-Tek mega-cassette	Sakura Finetek Japan Co., Ltd., Tokyo, Japan
Tissue-Tek O.C.T. compound	Sakura Finetek Japan Co., Ltd., Tokyo, Japan
Triton X-100	Nacalai Tesque, Kyoto, Japan
TRIzol reagent	Invitrogen, Carlsbad, CA, USA
Tween-20	ChemCruz, Santa Cruz Biotechnology, Dalla
Vancomycin hydrochloride	FUJIFILM Wako Pure Chemical Corporation, Osaka, Japan
Xylene	Nacalai Tesque, Kyoto, Japan

Table 4. Sample information on MASH patients

ID	Liver biopsy	HCC	Age	BW (kg)	BMI
MASH1	Matteoni 4	+	69	57.9	26.1
MASH2	Matteoni 4	+	56	66.4	25.9
MASH3	Matteoni 4	-	77	71.3	35.4
MASH4	Matteoni 4	-	67	64.5	29.4
MASH5	Matteoni 4	-	64	67.4	32.1
MASH6	Matteoni 4	-	60	50.1	23.2
MASH8	Matteoni 4	+	66	98.8	35.0
MASH9	Matteoni 4	+	79	65.2	29.0
MASH10	Matteoni 3	-	49	79.5	27.5

Table 5. Information on HD *vs* MASH patients

	HD (n=12)	**MASH (n=10)**	***P* value**
Age (years), median (min–max)	49 (26–64)	65 (49–79)	0.0008
Gender (male/female)	3/9	4/6	0.652
BMI (kg/m^2), median (min–max)	21 (19–24)	29 (23–35)	<0.0001

Table 6. MASH patients' characteristics-Medical History

Patient ID	DM (Y/N)	HTN (Y/N)	DLP (Y/N)	PPI	Anti-DM drug	Anti-HTN drug
MASH 1	Y	N	N	rabeprazole	N	N
MASH 2	Y	Y	N	lansoprazole	insulin	candesartan
MASH 3	Y	Y	Y	N	metformin, sitagliptin, glimepiride	benidipine, trichlormethiazide, olmesartan, azelnidipine
MASH 4	Y	N	N	rabeprazole	metformin, repaglinide	N
MASH 5	Y	Y	Y	rabeprazole	glimepiride, voglibose	candesartan, trichlormethiazide, amlodipine
MASH 6	N	N	Y	N	N	N
MASH 7	Y	Y	N	esomeprazole	metformin	irbesartan, amlodipine
MASH 8	Y	Y	N	N	sitagliptin, mitiglinide, voglibose	amlodipine
MASH 9	N	N	N	rabeprazole	-	N
MASH 10	Y	N	N	esomeprazole	linagliptin	N

DM: Diabetes Mellitus; HTN: Hypertension; DLP: Dyslipidemia; PPI: Proton Pump Inhibit

Table 7. MASH patients' characteristics-Biochemical and Blood Tests and Others

Patient ID	WBC (/μL)	Neu (/μL)	PLT (x10^4/μL)	Hb (g/dl)	FPG (mg/dl)	HbA1c (%)	Albumin (g/dl)	HCV_ Ab	AFP (ng/ml)
MASH 1	4.32	2.93	5.5	11.5	122	5.7	3.8	-	4.9
MASH 2	4.31	2.41	6.2	14.7	144	7.5	3.9	-	4
MASH 3	7.33	4.97	11	14.4	162	7	4.4	-	3

MASH 4	3.61	1.98	8.8	12.4	129	5.5	3.8	-	6
MASH 5	6.06	3.3	26.9	11.9	108	6.1	4	-	5
MASH 6	4.08	2.57	20.6	14.1	101	5.5	4	-	3
MASH 7	7.11	5.12	14.1	14.5	130	9.4	4.4	-	-
MASH 8	6.86	4.29	16.6	12.7	128	7.9	3.6	-	91
MASH 9	1.5	0.44	7	8.8	106	4.4	2.5	-	4880
MASH 10	2.9	1.63	5.3	13.3	84	6.3	4.5	-	6

Neu: Neutrophil; PLT: Platelet; Hb: Hemoglobin; FPG: Fasting plasma glucose; HCV: Hepatitis C Virus; AFP: Alpha-Fetoprotein

Table 8. MASH patients' characteristics-Liver Function Tests and Lipid Profile

Patient ID	AST (IU/L)	ALT (IU/L)	GGT (IU/L)	ALP (IU/L)	T-Bil (mg/dl)	TC (mg/dl)	LDL-C (mg/dl)	HDL-C (mg/dl)	TG (mg/dl)
MASH 1	36	29	113	453	1.2	166	86	70	49
MASH 2	27	25	51	404	1.2	100	35	47	93
MASH 3	74	74	102	170	0.9	147	94	35	91
MASH 4	39	46	57	357	0.9	133	68	45	100
MASH 5	34	31	29	151	0.6	170	92	50	143
MASH 6	50	64	57	227	0.6	174	117	45	63
MASH 7	134	147	201	543	0.8	179	98	54	133
MASH 8	36	48	100	254	0.7	188	139	24	123
MASH 9	48	35	127	518	1.3	120	74	41	24
MASH 10	36	34	70	251	1.1	170	102	50	90

AST: Aspartate Aminotransferase; ALT: Alanine Aminotransferase; GGT: Gamma-Glutamyl Transferase; ALP: Alkaline Phosphatase; T-Bil: Total bilirubin; TC: Total cholesterol; LDL-C: Low-Density Lipoprotein Cholesterol; HDL-C: High-Density Lipoprotein Cholesterol; TG: Triglycerides

Table 9. MASH patients' characteristics-Liver imaging/Pathology

Patient ID	FibroScan Stiffness (kPa)	Matteoni (1-4)	NAS (0-8)	NAS Ballooning (0-2)	NAS Steatosis (0-3)	NAS Inflammation (0-8)	Fibrosis stage (F0–F4)
MASH 1	-	4	4	1	2	1	F4
MASH 2	12.2	4	3	1	1	1	F3
MASH 3	17.1	4	6	2	2	2	F3
MASH 4	26.3	4	5	2	2	1	F4

MASH 5	7.8	4	4	1	2	1	F3
MASH 6	7.9	4	5	1	3	1	F3
MASH 7	16.9	4	4	1	1	2	F3
MASH 8	20.5	4	3	1	1	1	F4
MASH 9	37.6	4	3	1	1	1	F4
MASH 10	19.6	3	3	1	1	1	F4

NAS: Histology NAFLD Activity Score

Matteoni 1, Simple steatosis (fat accumulation in hepatocytes), no evidence of inflammation

Matteoni 2: Steatosis with lobular inflammation, no ballooning of hepatocytes or fibrosis

Matteoni 3: Steatosis with ballooning hepatocyte degeneration, no fibrosis present

Matteoni 4: Steatosis with ballooning hepatocyte degeneration, lobular inflammation and fibrosis

Table 10. the composition of SD diet and CDAHFD diet

Product #	**A06071314 (SD diet)**	**A06071302 (CDAFHD diet)**
Ingredient	**gm**	**gm**
L-Methionine	5.1	0.8
Choline Bitartrate	2	0
Corn Starch	502	0
FD&C Yellow Dye #5	0.04	0
FD&C Red Dye #40	0	0.025
FD&C Blue Dye #1	0.01	0.025
Total	**1039.35**	**756.05**
kcal %		
Protein	18	18
Carbohydrate	71	20
Fat	10	62
Total	100	100
kcal / gm	3.8	5.2

Methods

Bacterial extraction from human stool samples

Bacteria were extracted from the human stool samples in an anaerobic chamber (Coy Laboratory Products). All reagents used in the anaerobic chamber were sterilized through a 0.22 μm filter (BMBio) and left in the anaerobic chamber overnight. The frozen stool samples were thawed, suspended in 30 ml of PBS, and centrifuged at 50 × g for 15 minutes at 4℃. The supernatant of each stool sample was collected and suspended thoroughly in PBS and then dispensed into 1 ml aliquots in 1.5 ml tubes. These were stored at -80℃ as bacterial frozen stocks of human stool samples.

Measurement of bacterial cell numbers in bacterial frozen stocks of human stool samples

Bacterial frozen stocks from human stool samples were thawed in an anaerobic chamber. Ten μl of the bacterial frozen stock was diluted 1,000-fold with PBS. The bacterial cell number was measured according to the Cell Viability kit (BD) protocol. Thiazole orange (TO, BD) was used to detect bacteria. Liquid counting beads (987/μl, BD) and TO (final concentration 42 nM) were added to the diluted bacterial solution and the mixture was left on ice for 10 minutes. A total volume of 200 μl was prepared, consisting of 10 μl bacterial dilution, 5 μl counting beads, 2 μl TO, and 183 μl PBS. The bacterial count measurement solution was subjected to flow cytometry analysis (FACS) using a SONY SA3800 Analyzer (SONY). The bacterial cell number was calculated based on the ratio of the number of Counting Beads and bacteria detected in the analysis.

Analysis of the proportion of W27 IgA-bound bacteria in human stool samples

After measuring the number of bacteria in the stool samples as mentioned before, the bacteria in the human stool samples were adjusted to 6×10^6 cells/tube by adding PBS. Then, the samples were centrifuged at 8,000 × g for 5 minutes at 4°C, and the supernatant was removed. A hundred µl of PBS containing 20% normal rat serum (Wako) was added to the bacteria, and the mixture was incubated on ice for 20 minutes. After blocking, 6×10^6 cells were reacted with 15 µg of biotinylated-mouse IgA for 30 min on ice and after washed, reacted with streptavidin-PE/Cy7 (Biolegend) for 30 min on ice. Thereafter, bacteria were washed with 10% fetal bovine serum and EDTA (final concentration of 5 µM, Nacalai Tesque) -containing PBS (FACS) buffer (8,000 g, 5 min, 4 °C). Bacteria were reacted with TO, and the percentage of W27 IgA-bound bacteria was analysed by SONY Cell Sorter SH800 (SONY).

Sorting for IgA-bound and -unbound bacteria by magnetic cell sorting (MACS)

Bacterial numbers were calculated as described above. After blocking, 6×10^6 cells were reacted with 15 µg of biotinylated-mouse IgA for 30 min on ice. Bacteria were washed with FACS buffer (8,000 g, 5 min, 4 °C) and were reacted with 15 µl of Microbeads-Streptavidin (Milteny) for 30 min on ice. After washing, IgA-bound and -unbound bacteria were sorted by MACS according to LS column protocol (Milteny). W27 IgA-bound and -unbound bacteria were stained by TO and goat anti-mouse IgA-PE (Southern Biotech) for 20 min on ice. IgA-bound and -unbound bacteria fractions were separated by SONY Cell Sorter SH800 and confirmed that a recovery ratio was more than 80%.

Bacterial DNA extraction

Bacterial genomic DNA extraction was performed according to a previous report (22) with minor modification. In brief, bacteria were lysed in DNA Lysis buffer (50 mM Tris–HCl, 300 mM NaCl, 1 mM EDTA and 0.5% SDS) on bead smash with glass beads (GB-01, TOMY), and the lysate was incubated with proteinase K (0.2 mg/ml, Nacalai) overnight at 55 °C. Bacterial DNA was purified by phenol/chloroform/isoamyl alcohol extraction and ethanol precipitation. Finally, DNA was dissolved in ultra-pure distilled water (Invitrogen) and stored at -20 °C.

Sequencing and analysis of 16S ribosomal RNA

Bacterial DNA was amplified by polymerase chain reaction (PCR) targeting the V3-V4 variable region of 16S ribosomal RNA (rRNA) gene with the following program: preheating at 98 °C for 3 min; 30 cycles of denaturation at 98 °C for 10 s, annealing at 46 °C for 5 s and extension at 72 °C for 30 s; and a terminal extension at 72 °C for 5 min. The primers used for 16S rRNA sequence were as follows: 342Fw (5'-AATGATACGGCGACCACCGAGATCTACACTCTTTCCCTACACGACGCTCTTCCGATCT CTACGGGGGGCAGCAG-3'), 806Rv (5'-CAAGCAGAAGACGGCATACGAGATXXXXXXGTGACTGGAGTTCAGACGTGTGCTCTT CCGATCTGGACTACCGGGGTATCT-3'). XXXXXX represents the index nucleotide sequence. PCR product was purified with Fast Gene gel extraction kit (Nippon Genetics). Sequence analysis was performed by Myskin Corporation using Miseq Reagent Kit V3 (Illumina). The sequence data were analysed by Quantitative Insights into Microbial Ecology (Qiime) 2

software (ver. 2020–2). Denoising and trimming of sequences were used by DADA2. For the α-diversity, ASV number was calculated by Qiime2. For the β-diversity, principal coordinate analysis based on unweighted unifrac distance (PERMANOVA/adonis) was analysed by QIIME2. The differences in each group were analyzed by linear discriminant analysis effect size (LDA) analysis.

Calculation of IgA index

The calculation of IgA index was performed following previous reports (22). IgA binding ability is the ratio of IgA-bound bacteria to gut microbiota. Since IgA binding ability of the individual is different, $IgA_{\text{taxon abundance}}$ was calculated based on the relative abundance of each fraction. This was used to calculate the ratio of IgA-bound or -unbound bacteria ($IgA^{+}_{\text{taxon abundance}}$, $\text{-}IgA^{-}_{\text{taxon abundance}}$) for each individual, followed by the IgA index calculation. In this study, bacteria with median value of IgA index greater than 0 are considered to be strongly bound by IgA.

FACS to analyses the mouse IgA binding ability to bacteria

E. faecalis was cultured as described above. After measuring the cell number of bacteria by FACS, adjust the concentration to 5×10^5 cells/tube for *E. faecalis*. After the washing and blocking mentioned above, 15 μg of biotinylated mouse monoclonal IgA antibody was added to the bacteria and react on ice for 30 minutes. Using the same procedure, 20 μl of PE/Cyanine7-Streptavidin was added to the mixture, and then the mixture was incubated on ice for 20 minutes in the dark. After washing, FACS buffer and SYTO24 (final concentration 42 nM, Invitrogen) were added to the bacteria, and the mixture was incubated on ice for 10 minutes. The antibody binding ability was then analyzed using a SONY Cell Sorter SH800.

ELISA for mouse IgA binding assay against bacteria

After the cultivation of *E. faecalis*, bacteria were washed with PBS (8,000 g, 5 min, 4 °C). Bacteria were suspended in 0.05 M Na_2CO_3 and were coated on ELISA plates (Thermo Fisher) at a concentration of 1×10^8 cells/well for *E. faecalis*. After blocking, the relative binding ability of mouse IgA was detected with AP-conjugated goat anti-mouse IgA (Southern Biotech). After adding substrate solution, the optical density (O.D.) 405 nm values were measured by Tristar2 LB942 (BERTHOLD TECHNOLOGIES).

Bacterial growth inhibition experiment

E. faecalis was cultured as described above and diluted in 1,000-fold with medium. Twenty-five μl of PBS or mouse monoclonal IgA antibody (1 mg/ml) was added to 5 μl of *E. faecalis* bacterial solution and incubated at 37°C for 1 hour. After the reaction, 30 μl of medium was added and incubated at 37°C for 6 hours. After culture, the bacterial liquid was spread onto BHI medium with serial dilution, and the plates were cultured overnight at 37°C. And then the number of colonies was counted. Cell number at 0 hour was also counted by the same procedure.

Histopathologic examination

For haematoxylin and eosin staining (H&E staining), the liver tissue was fixed in 10% neutral formalin, embedded in paraffin, and cut into 4 μm-thick sections. For Oil Red O staining, liver tissue was fixed in 10% neutral formalin at least 24 hours, then gradient dehydrated by 10% ~

30% sucrose solution. After the dehydration, the liver tissue was frozen in compound (Sakura) and stored at -80℃. Ten μm cryostat sections were fixed in acetone at -20℃ for 10 minutes and then conduct the staining with Oil Red O staining kit (FUJIFILM). For Sirius Red staining, the liver tissue was fixed in 10% neutral formalin, embedded in paraffin, cut into 4 μm-thick sections, and stained with the Picro Sirius Red Stain Kit (ScyTek Laboratories).

Semi-quantification of Sirius red staining

For semi-quantification Sirius Red Staining, Image J 1.54 was used. We choose to calculate the full-size of the staining slides and excluded the surrounding portal vein areas. We change the image to RGB style and select the green channel, and then set the scale as "distance in pixels=700, known distance=1.00, pixel aspect ratio=1.0, unit of length=um", and set the threshold as (0, 180). We measured the percentages of red areas and performed the statistical analysis **(Fig. S6)**.

Quantitative real-time PCR (qPCR)

Frozen tissues were placed in tubes (2 mL) and homogenized in 1 mL of ISOGEN II (NIPPON GEN) and 200 μL of chloroform (Sigma). Samples were then centrifuged for 10 min at 13,000 × rpm for phase separation, and the upper aqueous phase of each sample was mixed in a 1:1 ratio with 70% ethanol. The samples were then applied to Qiagen RNeasy spin columns with reagents according to the manufacturer’s protocol. The purity and concentration of RNA were determined using a NanoDrop spectrophotometer (Thermo Fisher Scientific). cDNA was synthesized from 1 μg of total RNA using the One-Step qRT-PCR Kit (Thermo Fisher Scientific)

according to manufacturer's instructions and the TaqMan™ Gene Expression Assays (Thermo Fisher Scientific). The amplification program consisted of an initial denaturation at 95 °C for 3 mins, followed by 60 cycles of 98 °C for 10 s, 57 °C for 10 s, and 72 °C for 5 s, finally end at 4 °C. β*-actin* was used as the endogenous control. The relative expression levels of target genes, including *Tnfα, Il1b, Il6, Ccl2, Col1a1, Col4a1, Acta2, and Tgfb1*, were calculated using the 2^− ∆ ∆ Ct method. Primer sequences are listed in Supplementary Table 2.

Serum ALT measurement

Mice were sacrificed, and whole blood was collected from the orbital sinus into 1.5 ml tubes. The blood samples were left undisturbed at room temperature for 1 hour, and then centrifuged at 2,000 × g for 10 minutes at 4°C. The serum was carefully collected and stored at −80°C until further analysis. For ALT activity measurement, frozen sera were thawed slowly on ice for at least 1 hour until completely thawed. ALT activity was measured using the ALT Activity Assay Kit (MAK052, Merck) according to the manufacturer's standard protocol.

Metabolite extraction from liver

Metabolite extraction from liver tissue for comprehensive metabolomic profiling was performed using the slightly modified protocol of a previously established method.

Liquid chromatography-tandem mass spectrometry (LCMS) for amino acid measurement

In essence, we employed a triple-quadrupole mass spectrometer equipped with an electrospray ionization (ESI) ion source (LCMS-8060, Shimadzu Corporation) operated in both positive and negative-ESI and in multiple reaction monitoring (MRM) modes. Analyte separation was achieved on a Discovery HS F5-3 column (2.1 mm I.D.×150 mm L, 3 μm particle size; Sigma-Aldrich) through a gradient elution with mobile phase A (0.1% formate) and mobile phase B (acetonitrile containing 0.1% formate). The elution profile was as follows: 100:0 (0–5 min), 75:25 (5–11 min), 65:35 (11–15 min), 5:95 (15–20 min), and 100:0 (20–25 min), with a constant flow rate of 0.25 mL/min and a column oven set at 40 °C.

Quantitative and qualitative data analyses of targeted metabolome analysis

For the measurement of metabolites registered in our in-house compound library, we compared the measurement results of samples and corresponding standards and confirmed that the retention times were consistent. Chromatographic peak integrations and confirmation of signal specificity for target compounds were performed for IC-HR-MS and LC-MS/MS, respectively, using Trace Finder software (ver. 4.1, Thermo Fisher Scientific) and Lab Solutions software (ver. 5.113, Shimadzu). For IC-HR-MS data analysis, the Trace Finder compound identification and confirmation setup parameters included a molecular ion intensity threshold override of 10,000, S/N 5, and mass tolerance of 5 ppm. Isotope pattern analysis using a 90% fit threshold, 30% allowable relative intensity deviation, and 5 ppm mass deviation were also performed to ensure that the relative intensities of the M + 1 and/or M + 2 isotope peaks for each compound were consistent with the theoretical relative intensities. For LC-MS/MS analysis, chromatographic peaks obtained with compound-specific SRM channels

were integrated and manually reviewed. For a single target compound, one or more confirmatory SRM channels were set (if available) to confirm peak compound identification. Chromatograms were acquired using Lab Solutions (ver. 5.113, Shimadzu). Peak areas were determined using Data browser software. The obtained peak quantitation values for each compound were corrected for recovery by IS (MES and L-Met for IC-HR-MS and LC-MS/MS, respectively). For the tissue metabolome, peak area values were further corrected for weight.

Statistical analysis and visualization of the metabolomics data

Metabolite profiles were analysed using R software (version 4.2.0, R Foundation for Statistical Computing, Vienna, Austria). Differentially abundant metabolites between treatment groups were identified using one-way analysis of variance (ANOVA) followed by Tukey's post-hoc test for multiple comparisons, with a significance threshold of $P < 0.05$. Prior to analysis, metabolite data were normalized using log transformation and auto-scaling to ensure normal distribution. For visualization, a hierarchical clustering heatmap was constructed using the "heatmap" package (version 1.0.12). Metabolites showing significant differences ($P < 0.05$) across experimental conditions were included in the heatmap. The data were scaled and centered to have a mean of zero and unit variance across samples. Hierarchical clustering was performed using Euclidean distance and complete linkage methods for both rows (metabolites) and columns (samples). The colour scale represents z-score transformed values, with red indicating increased metabolite levels (positive z-scores) and blue indicating decreased levels (negative z-scores). The final heatmap was generated with a resolution of 600 dpi and exported in TIFF format for publication.

49 Spadina Ave. Suite 200
Toronto ON M5V 2J1 Canada
www.biorender.com

Confirmation of Publication and Licensing Rights

August 19th, 2025

Subscription Type:	*Student Plan - Academic*
Agreement number:	*PR28NG9624*
Publisher Name:	*hepatology*
Citation to Use:	*Created in BioRender. Ruopeng, W. (2025) https://BioRender.com/8p0z9nx*

To whom this may concern,

This document is to confirm that Wang Ruopeng has been granted a license to use the BioRender Content, including icons, templates, and other original artwork, appearing in the attached Completed Graphic pursuant to BioRender's Academic License Terms. This license permits BioRender Content to be sublicensed for use in publications (journals, textbooks, websites, etc.).

All rights and ownership of BioRender Content are reserved by BioRender. All Completed Graphics must be accompanied by the following citation: "Created in BioRender. Ruopeng, W. (2025) https://BioRender.com/8p0z9nx".

BioRender Content included in the Completed Graphic is not licensed for any commercial uses beyond use in a publication. For any commercial use of this figure, users may, if allowed, recreate it in BioRender under an Industry BioRender Plan.

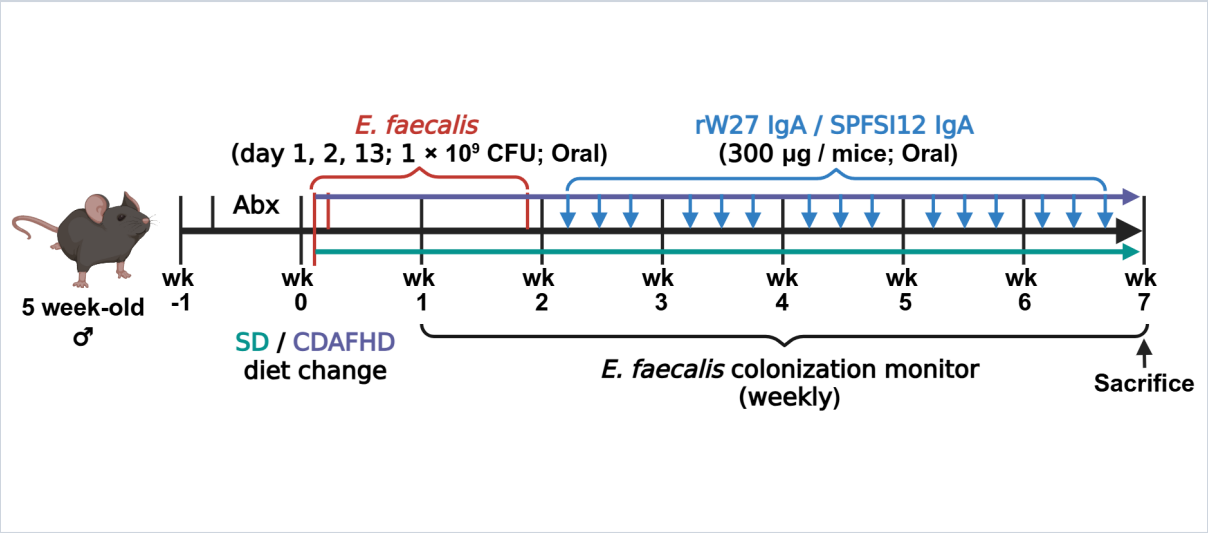

For any questions regarding this document, or other questions about publishing with BioRender, please refer to our BioRender Publication Guide, or contact BioRender Support at support@biorender.com.

49 Spadina Ave. Suite 200
Toronto ON M5V 2J1 Canada
www.biorender.com

Confirmation of Publication and Licensing Rights

August 19th, 2025

Subscription Type:	*Student Plan - Academic*
Agreement number:	*AH28NG99T4*
Publisher Name:	*hepatology*
Citation to Use:	*Created in BioRender. Ruopeng, W. (2025) https://BioRender.com/d5c32ha*

To whom this may concern,

This document is to confirm that Wang Ruopeng has been granted a license to use the BioRender Content, including icons, templates, and other original artwork, appearing in the attached Completed Graphic pursuant to BioRender's Academic License Terms. This license permits BioRender Content to be sublicensed for use in publications (journals, textbooks, websites, etc.).

All rights and ownership of BioRender Content are reserved by BioRender. All Completed Graphics must be accompanied by the following citation: "Created in BioRender. Ruopeng, W. (2025) https://BioRender.com/d5c32ha".

BioRender Content included in the Completed Graphic is not licensed for any commercial uses beyond use in a publication. For any commercial use of this figure, users may, if allowed, recreate it in BioRender under an Industry BioRender Plan.

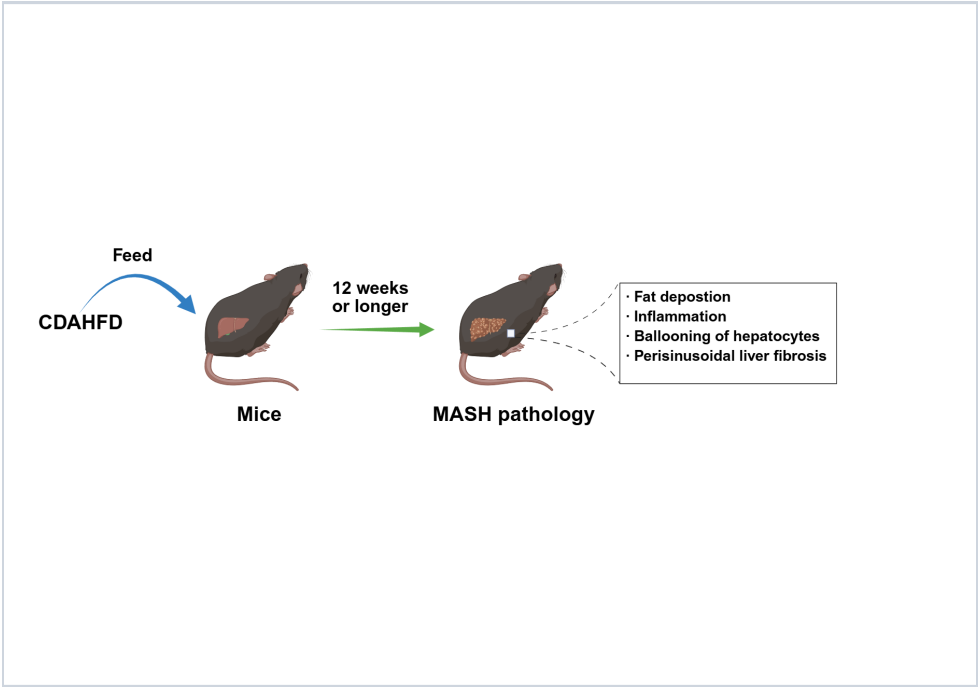

For any questions regarding this document, or other questions about publishing with BioRender, please refer to our BioRender Publication Guide, or contact BioRender Support at support@biorender.com.

49 Spadina Ave. Suite 200
Toronto ON M5V 2J1 Canada
www.biorender.com

Confirmation of Publication and Licensing Rights

August 19th, 2025

Subscription Type:	*Student Plan - Academic*
Agreement number:	*CF28NG901H*
Publisher Name:	*hepatology*
Citation to Use:	*Created in BioRender. Ruopeng, W. (2025) https://BioRender.com/j385gsk*

To whom this may concern,

This document is to confirm that Wang Ruopeng has been granted a license to use the BioRender Content, including icons, templates, and other original artwork, appearing in the attached Completed Graphic pursuant to BioRender's Academic License Terms. This license permits BioRender Content to be sublicensed for use in publications (journals, textbooks, websites, etc.).

All rights and ownership of BioRender Content are reserved by BioRender. All Completed Graphics must be accompanied by the following citation: "Created in BioRender. Ruopeng, W. (2025) https://BioRender.com/j385gsk".

BioRender Content included in the Completed Graphic is not licensed for any commercial uses beyond use in a publication. For any commercial use of this figure, users may, if allowed, recreate it in BioRender under an Industry BioRender Plan.

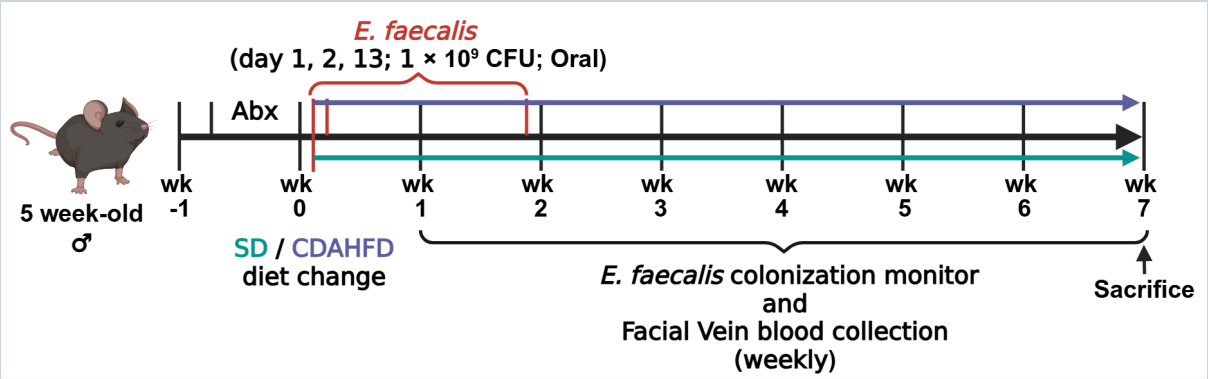

For any questions regarding this document, or other questions about publishing with BioRender, please refer to our BioRender Publication Guide, or contact BioRender Support at support@biorender.com.